Chapter

Nonlinear Schrödinger Equation

Jing Huang

Abstract

Firstly, based on the small-signal analysis theory, the nonlinear Schrodinger equation (NLSE) with fiber loss is solved. It is also adapted to the NLSE with the high-order dispersion terms. Furthermore, a general theory on cross-phase modulation (XPM) intensity fluctuation which adapted to all kinds of modulation formats (continuous wave, non-return-to-zero wave, and return-zero pulse wave) is presented. Secondly, by the Green function method, the NLSE is directly solved in the time domain. It does not bring any spurious effect compared with the split-step method in which the step size has to be carefully controlled. Additionally, the fourth-order dispersion coefficient of fibers can be estimated by the Green function solution of NLSE. The fourth-order dispersion coefficient varies with distance slightly and is about 0.002 ps^4/km, 0.003 ps^4/nm, and 0.00032 ps^4/nm for SMF, NZDSF, and DCF, respectively. In the zero-dispersion regime, the higher-order nonlinear effect (higher than self-steepening) has a strong impact on the short pulse shape, but this effect degrades rapidly with the increase of β_2. Finally, based on the traveling wave solution of NLSE for ASE noise, the probability density function of ASE by solving the Fokker-Planck equation including the dispersion effect is presented.

Keywords: small-signal analysis, Green function, traveling wave solution, Fokker-Planck equation, nonlinear Schrodinger equation

1. Introduction

The numerical simulation and analytical models of nonlinear Schrödinger equation (NLSE) play important roles in the design optimization of optical communication systems. They help to understand the underlying physics phenomena of the ultrashort pulses in the nonlinear and dispersion medium.

The inverse scattering [1], variation, and perturbation methods [2] could obtain the analytical solutions under some special conditions. These included the inverse scattering method for classical solitons [3], the dam-break approximation for the non-return-to-zero pulses with the extremely small chromatic dispersion [4], and the perturbation theory for the multidimensional NLSE in the field of molecular physics [5]. When a large nonlinear phase was accumulated, the Volterra series approach was adopted [6]. With the assumption of the perturbations, the NLSE with varying dispersion, nonlinearity, and gain or absorption parameters was solved in [7]. In [8], the generalized Kantorovitch method was introduced in the extended NLSE. By introducing Rayleigh's dissipation function in Euler-Lagrange equation,

the algebraic modification projected the extended NLSE as a frictional problem and successfully solved the soliton transmission problems [9].

Since the numerical computation of solving NLSE is a huge time-consuming process, the fast algorithms and efficient implementations, focusing on (i) an accurate numerical integration scheme and (ii) an intelligent control of the longitudinal spatial step size, are required.

The finite differential method [10] and the pseudo-spectral method [11] were adopted to increase accuracy and efficiency and suppress numerically induced spurious effects. The adaptive spatial step size-controlling method [12] and the predictor-corrector method [13] were proposed to speed up the implementation of split-step Fourier method (SSFM). The cubic (or higher order) B-splines were used to handle nonuniformly sampled optical pulse profiles in the time domain [14]. The Runge-Kutta method in the interaction picture was applied to calculate the effective refractive index, effective area, dispersion, and nonlinear coefficients [15].

Recently, the generalized NLSE, taking into account the dispersion of the transverse field distribution, is derived [16]. By an inhomogeneous quasi-linear first-order hyperbolic system, the accurate simulations of the intensity and phase for the Schrödinger-type pulse propagation were obtained [17]. It has been demonstrated that modulation instability (MI) can exist in the normal GVD regime in the higher-order NLSE in the presence of non-Kerr quintic nonlinearities [18].

In this chapter, several methods to solve the NLSE will be presented: (1) The small-signal analysis theory and split-step Fourier method to solve the coupled NLSE problem, the MI intensity fluctuation caused by SPM and XPM, can be derived. Furthermore, this procedure is also adapted to NLSE with high-order dispersion terms. The impacts of fiber loss on MI gain spectrum can be discussed. The initial stage of MI can be described, and then the whole evolution of MI can also be discussed in this way; (2) the Green function to solve NLSE in the time domain. By this solution, the second-, third-, and fourth-order dispersion coefficients is discussed; and (3) the traveling wave solution to solve NLSE for ASE noise and its probability density function.

2. Small-signal analysis solution of NLSE for MI generation

2.1 Theory for continuous wave

The NLSE governing the field in nonlinear and dispersion medium is

$$\frac{\partial u}{\partial z}+\beta_1\frac{\partial u}{\partial t}+\frac{i}{2}\beta_2\frac{\partial^2 u}{\partial t^2}+\frac{a}{2}u=i\gamma\left[|u|^2+2|u'|^2\right]u \tag{1}$$

where β_1 and β_2 are the dispersions, γ is the nonlinear coefficient, and α is the fiber loss. In the frequency domain, the solution is

$$u(z+dz,\omega)=\exp\left(dz\hat{D}\right)\exp\left(dz\hat{N}\right)u(z,\omega) \tag{2}$$

where $\hat{D}=\frac{i}{2}\omega^2\beta_2+i\omega\beta_1-\frac{a}{2}$ and $\hat{N}=i\gamma\left[|u|^2+i2|u'|^2\right]$ [19] (**Figure 1**).

Usually, the field amplitudes can be written as

$$u(z,\omega)=\sqrt{P(z,\omega)}\exp\left[i\phi(z,\omega)\right] \tag{3}$$

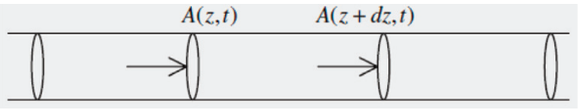

Figure 1.
Schematic illustration of medium. u(z, t) *and* u(z + dz, t) *correspond to the field amplitudes at* z *and* z + dz, *respectively.*

$\phi(z,\omega)$ is caused by the nonlinear effect, and $\phi(z,\omega) = \int_0^z \gamma[P(z,\omega) + 2P'(z,\omega)]dz$ [3].

$u(z+dz,\omega)$ (is)

$$\begin{aligned} u(z+dz,\omega) &= \exp\left(dz\hat{D}\right)\sqrt{P(z,\omega)}\exp\{i\varphi(z,\omega) + i\gamma[P+2P']dz\} \\ &= e^{-adz/2}\exp\left(\beta_1\omega dz\right)\exp\left(\beta_2/2\omega^2 dz\right)\sqrt{P(z,\omega)}e^{i\varphi(z+dz,\omega)} \\ &= \sqrt{P(z+dz,\omega)}\exp\left[i\varphi(z+dz.\omega)\right] \end{aligned} \tag{4}$$

Assuming: $P(z,\omega) = \langle P(z)\rangle + \Delta P(z,\omega)$

$\langle P(z)\rangle$ is the average signal intensity. $\Delta P(z,\omega)$ is the noise or modulation term. There is [20] $\langle P(z)\rangle\, \Delta P(z,\omega)$

The amplitude $\sqrt{P(z,\omega)}$ can be regarded as

$$\sqrt{P(z,\omega)} \approx \sqrt{\langle P(z)\rangle}\left(1 + \frac{\Delta P(z,\omega)}{2P(z)}\right) \tag{5}$$

The small-signal theory implies that the frequency modulation or noise $\dot{\varphi}(z+dz,\omega) = \frac{d\dot{\varphi}(z+dz,\omega)}{dt}$ is small enough. Finally ([21])

$$\begin{aligned} P(z+dz,\omega) &= \langle P(z)\rangle + 2e^{-adz/2}\times \\ &\quad \mathrm{Re}\left\{\langle P(z)\rangle\exp\left(i\omega\beta_1 dz + i\omega^2\beta_2 dz\right)\left[\frac{\Delta P(z,\omega)}{2\langle P(z)\rangle} + i\varphi(z+dz,\omega)\right]\right\} \end{aligned} \tag{6}$$

The operation $\exp\left(i\omega\beta_1 dz + i\omega^2\beta_2 dz\right)$ can be split into its real and imaginary parts:

$$\exp\left(i\omega\beta_1 dz + i\omega^2\beta_2 dz\right) = \cos\left(\omega\beta_1 dz + \omega^2\beta_2 dz\right) + i\sin\left(\omega\beta_1 dz + \omega^2\beta_2 dz\right) \tag{7}$$

The modulation or noise $\Delta P(z+dz,\omega)$ is $\Delta P(z+dz,\omega) \approx P(z+dz,\omega) - \langle P(z)\rangle$

So

$$\begin{aligned} P(z+dz,\omega) &= e^{-adz/2 - i\omega\beta_1 dz} \\ &\quad \left[\cos\left(\frac{1}{2}\beta_2\omega^2 dz\right)\Delta P(z,\omega) + \sin\left(\frac{1}{2}\beta_2\omega^2 dz\right)2\langle P(z)\rangle\varphi(z+dz,\omega)\right] \end{aligned} \tag{8}$$

And

$$\begin{pmatrix} \dfrac{\Delta P(z+dz,\omega)}{2\langle P(z)\rangle} \\ \varphi(z+dz,\omega) \end{pmatrix} = e^{-adz/2-i\omega\beta_1 dz} e^{i\gamma[\langle P(z)\rangle+2\langle P'(z)\rangle]dz} \begin{pmatrix} \cos\left(\frac{1}{2}\beta_2\omega^2 dz\right) & -\sin\left(\frac{1}{2}\beta_2\omega^2 dz\right) \\ \sin\left(\frac{1}{2}\beta_2\omega^2 dz\right) & \cos\left(\frac{1}{2}\beta_2\omega^2 dz\right) \end{pmatrix} \begin{pmatrix} \dfrac{\Delta P(z,\omega)}{2\langle P(z)\rangle} \\ \varphi(z,\omega) \end{pmatrix} \tag{9}$$

When only intensity modulation is present and no phase modulation exists, the transfer function $\cos\left(\frac{1}{2}\beta_2\omega^2 dz\right)$ is obtained. The 3 dB cutoff frequency corresponds to $\frac{1}{2}\beta_2\omega^2 dz = \pi/4$ in [22, 23]. This treatment is also adaptable to the case that only the nonlinear phase (frequency) modulation is present; then, the intensity modulation $\Delta P(z+dz,\omega)$ due to FM-IM conversion is given as

$$\Delta P(z+dz,\omega) = 2\langle P(z)\rangle e^{-adz/2-i\omega\beta_1 dz} \sin\left(\frac{1}{2}\beta_2 dz\omega^2\right)\varphi(z+dz,\omega) \tag{10}$$

This is in very good agreement with [24] for small-phase modulation index. Even for large modulation index $\frac{1}{2}\beta_2\omega^2 dz = \pi/2$, the difference is within 0.5 dB. Eq. (10) does not include a Bessel function, so it is simpler than that in [24].

Obviously, the above process can be used to treat NLSE with higher-order dispersion (β_3, β_4) [25]. Similarly, the result in Eq. (10) will include ω^3 and ω^4.

The corresponding MI gain g_{MI} in the side bands of ω_0 (the frequency of signal) is given by

$$\begin{aligned} g_{MI}(z,\omega) &= \frac{|\Delta P(z+dz,\omega)-\Delta P(z,\omega)|}{\langle P(z)\rangle dz} \\ &= 2e^{-adz/2-i\omega\beta_1 dz}\sin\left(\frac{1}{2}\beta_2 dz\omega^2\right)\left\{\gamma\int_z^{z+dz}[P(z,\omega)+2P'(z,\omega)]dz\right\}\Big/dz \end{aligned} \tag{11}$$

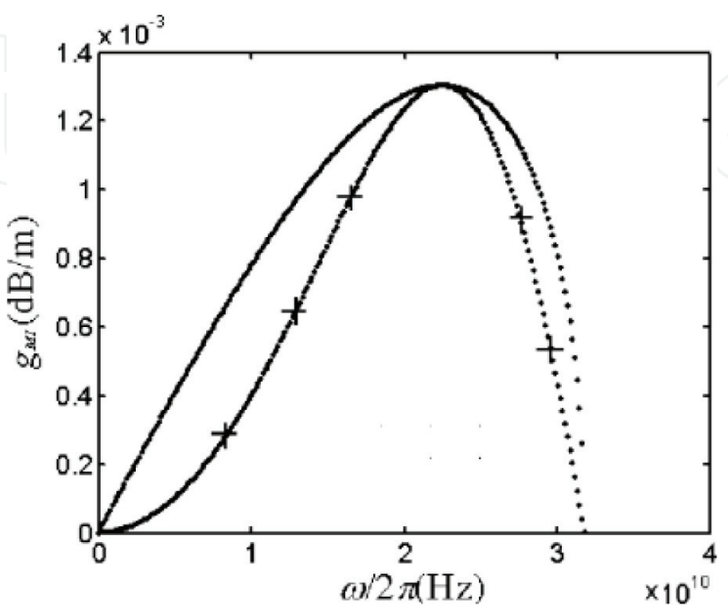

Figure 2.
MI gain spectra. +++ result of small-signal analysis. —— result of perturbation approach. The parameters are P_0 = 10 dBm, β_2 = 15 ps^2/km, λ = 1550 nm, a = 0.21 dB/km, γ = 0.015W^{-1}/m, and z = 0 m.

Figure 2 shows a comparison of the gain spectra between Eq. (11) and [6] for the case $\langle P(z)\rangle/\langle P'(z)\rangle = 1$. The maximum frequency modulation index caused by dispersion corresponds to $\frac{1}{2}\beta_2\omega^2 dz = \pi$ [22, 23], and the maximum value of the sideband is $\omega_c = \sqrt{4\gamma\langle P(z)\rangle/|\beta_2|}$, so the choice of dz satisfies $\frac{1}{2}\beta_2\omega^2 dz = \pi$, which makes Eq. (11) have the same frequency regime as [26]. In **Figure 2**, the curves are different but have the same maximum value of g_{MI}. In practice, researchers generally utilize the maximum value of g_{MI} to estimate the amplified noises and SNR [3]. The result of small-signal analysis in **Figure 2** has a phase delay of around ω_0. Compared with the experiment result of [27], the reason is taking the fiber loss into account, the gain spectrum exhibits a phase delay close to ω_0, and the curve descends a little [27]. Fiber loss results in the difference of g_{MI} between the small-signal analysis method and the perturbation approach.

2.2 The general theory on cross-phase modulation (XPM) intensity fluctuation

For the general case of two channels, the input optical powers are denoted by $P(t), P'(t)$, respectively [28]. Only in the first walk-off length, the nonlinear interaction (XPM) is taken into account; in the remaining fibers, signals are propagated linearly along the fibers, and dispersion acts on the phase-modulated signal resulting in intensity fluctuation. According to [4], the whole length L is separated into two parts $0 < z < L_{wo}$ and $L_{wo} < z < L$; L_{wo} is the walk-off length, $L_{wo} = \Delta t/(D\Delta\lambda)$. Δt is the edge duration of the carrier wave, D is the dispersion coefficient, and $\Delta\lambda$ is the wavelength spacing between the channels. By the small-signal analysis, the phase modulation in channel 1 originating in dz at z can be expressed as

$$d\phi_{XPM}(z,t) = \gamma 2P'\left(z, t - z\beta_1'\right)e^{-az}dz \tag{12}$$

This phase shift is converted to an intensity fluctuation through the group velocity dispersion (GVD) from z to the receiver. So, at the fiber output, the intensity fluctuation originating in dz in the frequency domain is given by [29].

$$\begin{aligned} dP_{XPM}(z,\omega) &= 2\left[e^{i\omega z\beta_1}P(z,\omega)\right]\otimes\left\{e^{-a(L-z)}\cdot e^{i\omega\beta_1(L-z)}\sin\left[b(L-z)\right]d\varphi_{XPM}(z,\omega)\right\} \\ &= 4\gamma\left[e^{i\omega z\beta_1}P(z,\omega)\right]\otimes\left\{e^{-a(L-z)}\cdot e^{-az}\cdot e^{i\omega\beta_1' z}\cdot e^{i\omega\beta_1(L-z)}P'(z,\omega)\sin\left[b(L-z)\right]\right\}dz \end{aligned} \tag{13}$$

$\otimes$ representing the convolution operation $b = \omega^2 D\lambda^2/(4\pi c)$, where c is the speed of light. At the fiber output, the XPM-induced intensity fluctuation is the integral of Eq. (13) with z ranging from 0 to L:

$$\begin{aligned} P_{XPM} &= \int_0^L dP_{XPM}(z,\omega)dz \\ &= \int_0^L 4\gamma\left[e^{i\omega z\beta_1}P(z,\omega)\right]\otimes\left\{e^{-a(L-z)}\cdot e^{-az}\cdot e^{i\omega\beta_1' z}\cdot e^{i\omega\beta_1(L-z)}P'(z,\omega)\sin\left[b(L-z)\right]\right\}dz \end{aligned} \tag{14}$$

The walk-off between co-propagating waves is regulated by the convolution operation.

3. Green function method for the time domain solution of NLSE

3.1 NLSE including the resonant and nonresonant cubic susceptibility tensors

From Maxwell's equation, the field in fibers satisfies

$$\nabla^2 \vec{E} - \frac{1}{c^2}\frac{\partial^2 \vec{E}}{\partial t^2} = -u_0 \frac{\partial^2 \vec{P_L}}{\partial t^2} - u_0 \frac{\partial^2 \vec{P_{NL}}}{\partial t^2} \tag{15}$$

$$\begin{aligned} \vec{P_L}\left(\vec{r},t\right) &= \varepsilon_0 \int_{-\infty}^{+\infty} \chi^{(1)}(t-t')\, \vec{E}\left(\vec{r},t'\right) dt' \\ &= \varepsilon_0 \int_{-\infty}^{+\infty} \chi^{(1)}(\omega)\, \vec{E}\left(\vec{r},\omega\right) \exp(i\omega t) d\omega \end{aligned} \tag{16}$$

$$\chi^{(1)}(\omega) = \int_{-\infty}^{+\infty} d\tau \chi^{(1)}(\tau) \exp(-j\omega\tau) \tag{17}$$

where $\vec{E}$ is the vector field and $\chi^{(1)}$ is the linear susceptibility. $\vec{P_L}$ and $\vec{P_{NL}}$ represent the linear and nonlinear induced fields, respectively [30]. The cubic susceptibility tensor including the resonant and nonresonant terms is

$$\chi^{(3)}(\omega) = \chi^{(3)}_{NR} + \chi^{(3)}_{R}(\omega) \tag{18}$$

There are

$$\begin{aligned} \vec{P}_{NL,NR}\left(\vec{r},t\right) &= \varepsilon_0 \iiint_{\infty} dt_1 dt_2 dt_3 \chi^{(3)}_{NR}(t_1,t_2,t_3) \vdots \vec{E}\left(\vec{r},t-t_1\right) \cdot \vec{E}\left(\vec{r},t-t_2\right) \cdot \vec{E}\left(\vec{r},t-t_3\right) \\ &= \varepsilon_0 \iiint_{\infty} d\omega_1 d\omega_2 d\omega_3 \chi^{(3)}_{NR}(-\omega_1-\omega_2-\omega_3;\omega_1+\omega_2+\omega_3) \\ &\quad \vec{E}\left(\vec{r},t_1\right) \cdot \vec{E}\left(\vec{r},t_2\right) \cdot \vec{E}\left(\vec{r},t_3\right) \exp(j\omega t)\delta(\omega-\omega_1-\omega_2-\omega_3) \end{aligned} \tag{19}$$

$$\begin{aligned} \chi^{(3)}_{NR}(-\omega_1-\omega_2-\omega_3;\omega_1+\omega_2+\omega_3) &= \iiint_{\infty} dt_1 dt_2 dt_3 \chi^{(3)}_{NR}(t_1,t_2,t_3) \\ &\quad \exp(-j\omega_1 t_1 - j\omega_2 t_2 - j\omega_3 t_3) \end{aligned} \tag{20}$$

$$\begin{aligned} \vec{P}_{NL,R}\left(\vec{r},t\right) &= \varepsilon_0 \iiint_{\infty} dt_1 dt_2 dt_3 \chi^{(3)}_{R}(t,t_1,t_2,t_3) \vdots \vec{E}\left(\vec{r},t-t_1\right) \cdot \vec{E}\left(\vec{r},t-t_2\right) \cdot \vec{E}\left(\vec{r},t-t_3\right) \\ &= \varepsilon_0 \iiint_{\infty} d\omega_1 d\omega_2 d\omega_3 \chi^{(3)}_{R}(t,-\omega_1-\omega_2-\omega_3;\omega_1+\omega_2+\omega_3) \\ &\quad \vec{E}\left(\vec{r},t_1\right) \cdot \vec{E}\left(\vec{r},t_2\right) \cdot \vec{E}\left(\vec{r},t_3\right) \exp(j\omega t)\delta(\omega-\omega_1-\omega_2-\omega_3) \end{aligned} \tag{21}$$

$$\begin{aligned} \chi^{(3)}_{R}(t) &= \frac{1}{\sqrt{2\pi}} \int_{-\infty}^{+\infty} \frac{a}{\omega-(\omega_1+\omega_2+\omega_3)+i\Gamma} e^{-i\omega t} d\omega \\ &= -\sqrt{\frac{\pi}{2}} a \left(1+\frac{\Gamma}{|\Gamma|}\right) e^{-|\Gamma|t+i(\omega_1+\omega_2+\omega_3)t-i\frac{\pi}{2}} \end{aligned} \tag{22}$$

Γ and a are the attenuation and absorption coefficients, respectively [31].
Repeating the process of [3]
$E = F(x,y)A(z,t)\exp(i\beta z)$, there is

$$\frac{\partial A}{\partial z}+\frac{i}{2}\beta_2\frac{\partial^2 A}{\partial t^2}-\frac{1}{6}\beta_3\frac{\partial^3 A}{\partial t^3}=-\frac{a}{2}A+i\frac{3k_0}{8nA_{eff}}\chi_{NR}^{(3)}|A|^2A+\frac{ik_0g(\omega_0)[1-if(\omega_0)]}{2nA_{eff}}A\int_{-\infty}^{t}\chi_R^{(3)}(t-\tau)|A(\tau)|^2d\tau \tag{23}$$

$k_0=\omega_0/c$, where ω_0 is the center frequency. A_{eff} is the effective core area. n is the refractive index. The last term is responsible for the Raman scattering, self-frequency shift, and self-steepening originating from the delayed response:

$$f(\omega_1+\omega_2+\omega_3)=\frac{2(\omega_1+\omega_2+\omega_3)(1-|\Gamma|)}{-2(\omega_1+\omega_2+\omega_3)^2-2|\Gamma|+|\Gamma|^2} \tag{24}$$

$$g(\omega_1+\omega_2+\omega_3)=\left[-2(\omega_1+\omega_2+\omega_3)^2-2|\Gamma|+|\Gamma|^2\right] \tag{25}$$

where $g(\omega_1+\omega_2+\omega_3)$ is the Raman gain and $f(\omega_1+\omega_2+\omega_3)$ is the Raman non-gain coefficients.

3.2 The solution by Green function

The solution has the form

$$A(z,t)=\varphi(t)e^{-iEz} \tag{26}$$

Then, there is

$$\frac{1}{2}\beta_2\frac{\partial^2\phi}{\partial t^2}+\frac{i}{6}\beta_3\frac{\partial^3\phi}{\partial t^3}-\frac{3k_0}{8nA_{eff}}\chi_{NR}^{(3)}|\phi|^2\phi-\frac{k_0g(\omega_s)[1-if(\omega_s)]}{2nA_{eff}}\phi\int_{-\infty}^{+\infty}\chi_R^{(3)}(t-\tau)|\phi(\tau)|^2d\tau=E\phi \tag{27}$$

Let

$$\hat{H}_0(t)=\frac{1}{2}\beta_2\frac{\partial^2}{\partial t^2}+\frac{i}{6}\beta_3\frac{\partial^3}{\partial t^3} \tag{28}$$

$$\hat{V}(t)=\frac{-3k_0}{8nA_{eff}}\chi_{NR}^{(3)}|\phi|-\frac{k_0g(\omega_s)[1-if(\omega_s)]}{2nA_{eff}}\int_{-\infty}^{+\infty}\chi_R^{(3)}(t-\tau)|\phi(\tau)|^2d\tau \tag{29}$$

and taking the operator $\hat{V}(t)$ as a perturbation item, we first solve the eigen equation $-\sum_{n=2}^{k}\frac{i^n}{n!}\beta_n\frac{\partial^n\varphi}{\partial T^n}=E\varphi$.

$$\frac{1}{2}\beta_2\frac{\partial^2\phi}{\partial T^2}+\frac{i}{6}\beta_3\frac{\partial^3\phi}{\partial T^3}=E\phi \tag{30}$$

Assuming $E=1$, we get the corresponding characteristic equation:

$$-\frac{1}{2}\beta_2r^2+\frac{\beta_3}{6}r^3=E \tag{31}$$

Its characteristic roots are r_1, r_2, r_3. The solution can be represented as

$$\phi=c_1\phi_1+c_2\phi_2+c_3\phi_3 \tag{32}$$

where $\phi_m = \exp(ir_m t)$, $m = 1, 2, 3$ and c_1, c_2, c_3 are determined by the initial pulse. The Green function of (30) is

$$\left(E - \hat{H}_0(t)\right) G_0(t,t') = \delta(t-t') \tag{33}$$

By the construction method, it is

$$G_0(t,t') = \begin{cases} a_1\varphi_1 + a_2\varphi_2 + a_3\varphi_3, & t>t' \\ b_1\varphi_1 + b_2\varphi_2 + b_3\varphi_3, & t<t' \end{cases} \tag{34}$$

At the point $t = t'$, there are

$$a_1\phi_1(t') + a_2\phi_2(t') + a_3\phi_3(t') = b_1\phi_1(t') + b_2\phi_2(t') + b_3\phi_3(t') \tag{35}$$

$$a_1\phi_1'(t') + a_2\phi_2'(t') + a_3\phi_3'(t') = b_1\phi_1'(t') + b_2\phi_2'(t') + b_3\phi_3'(t') \tag{36}$$

$$a_1\phi_1''(t') + a_2\phi_2''(t') + a_3\phi_3''(t') - b_1\phi_1''(t') - b_2\phi_2''(t') - b_3\phi_3''(t') = -6i/\beta_3 \tag{37}$$

Let $b_1 = b_2 = b_3 = 0$, then

$$a_1 = \frac{\varphi_2\dot{\varphi}_3 - \dot{\varphi}_2\varphi_3}{W(t')}, a_2 = \frac{\varphi_3\dot{\varphi}_1 - \dot{\varphi}_3\varphi_1}{W(t')}, a_3 = \frac{\varphi_1\dot{\varphi}_2 - \dot{\varphi}_1\varphi_2}{W(t')} \tag{38}$$

$$W(t') = \begin{vmatrix} \phi_1 & \phi_2 & \phi_3 \\ \phi_1^{(1)} & \phi_2^{(1)} & \phi_3^{(1)} \\ \phi_1^{(2)} & \phi_2^{(2)} & \phi_3^{(2)} \end{vmatrix} \tag{39}$$

Finally, the solution of (27) can be written with the eigen function and Green function:

$$\begin{aligned} \varphi(t) &= \phi(t) + \int G_0(t,t')V(t')\varphi(t')dt' \\ &= \phi(t) + \int G_0(t,t',E)V(t')\phi(t')dt' + \int dt' G_0(t,t',E)V(t')\int G_0(t',t'',E)V(t'')\varphi(t'')dt'' \\ &= \phi(t) + \int G_0(t,t',E)V(t')\phi(t')dt' + \int dt' G_0(t,t',E)V(t')\int G_0(t',t'',E)V(t'')\phi(t'')dt'' + \cdots \\ &\quad + \underbrace{\int dt' G_0(t,t')V(t')\int G_0(t',t'')V(t'')dt''\cdots}_{\text{times } l}\int G_0(t^l,t^{l+1})V(t^{l+1})\varphi(t^{l+1})dt^{l+1} \end{aligned} \tag{40}$$

The accuracy can be estimated by the last item of (40). The algorithm is plotted in **Figure 3**.

3.3 Estimation of the fourth-order dispersion coefficient β_4

The NLSE governing the wave's transmission in fibers is

$$\frac{\partial u}{\partial z} + \frac{i}{2}\beta_2\frac{\partial^2 u}{\partial t^2} - \frac{1}{6}\beta_3\frac{\partial^3 u}{\partial t^3} - i\gamma\exp(-2\alpha z)\left[|u|^2 u + is\frac{\partial|u|^2}{\partial t}u + is|u|^2\frac{\partial u}{\partial t}\right] = 0 \tag{41}$$

where s is the self-steepening parameter. In the frequency domain, its solution is

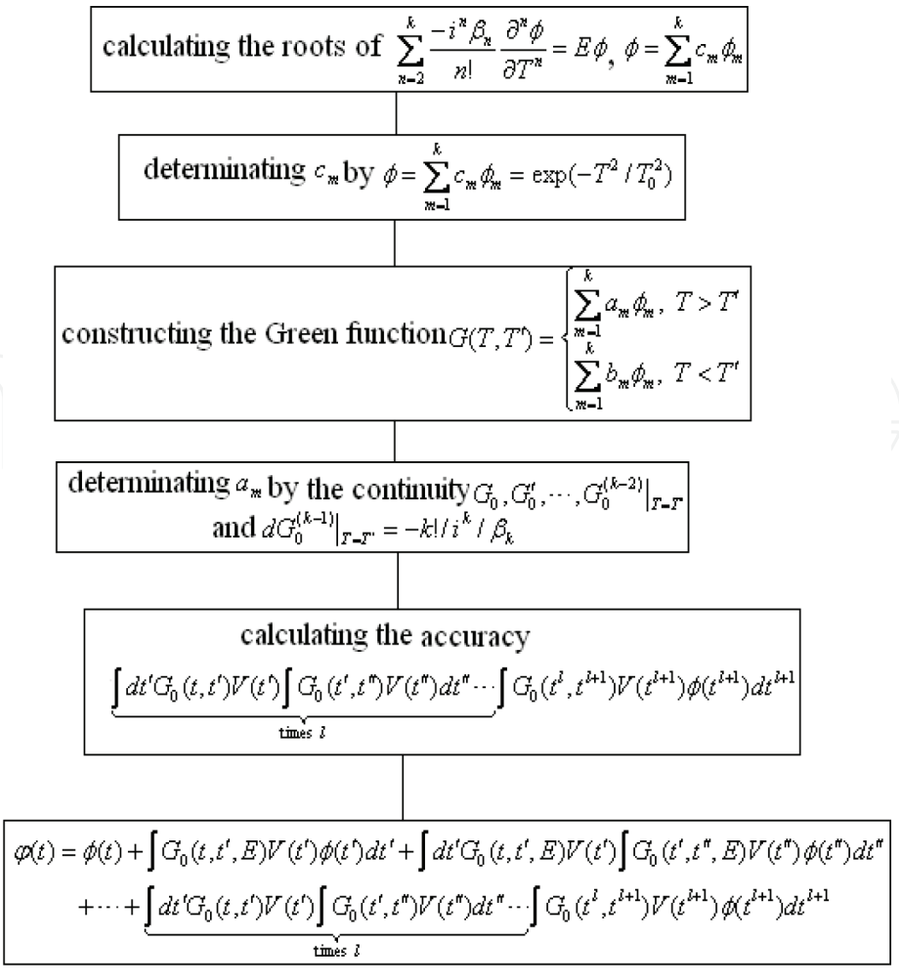

Figure 3.
The Green algorithm for solving NLSE.

$$u(z+dz,\omega)=\exp\left(dz\hat{D}\right)\exp\left(dz\hat{N}\right)u(z,\omega) \tag{42}$$

where $\hat{D}=\frac{i}{2}\omega^2\beta_2-\frac{i}{6}\omega^3\beta_3$, $\hat{N}=\Gamma\left\{i\gamma\exp(-2\alpha z)\left[|u|^2+is\frac{\partial|u|^2}{\partial t}+is|u|^2\frac{\partial}{\partial t}\right]\right\}$, and Γ represents the Fourier transform [32]. Let $\hat{L}=\frac{\partial}{\partial z}-\hat{D}-\hat{N}$ and $\hat{L}G(z,z',\omega)=\delta(z-z')$; we obtain the Green function

$$G\left(z,z',\omega\right)=\frac{1}{2\pi}\int_{-\infty}^{+\infty}\frac{\exp\left[-ik\left(z-z'\right)\right]}{ik-\hat{D}-\hat{N}}dk \tag{43}$$

Constructing the iteration $\beta_3=\beta_3^0+\delta\beta_3$, $u(z,\omega)=u^0(z,\omega)+\delta u(z,\omega)$, then there is

$$\delta u(z,\omega)=\int G\left(z,z',\omega\right)Z\left(z',\omega,\delta\beta_3\left(z'\right),u^0\left(z',\omega\right)\right)dz' \tag{44}$$

where $Z\left(z',\omega,\delta\beta_3\left(z'\right),u^0\left(z',\omega\right)\right)=-\frac{i}{6}\delta\beta_3\left(z'\right)\omega^3u^0\left(z',\omega\right)$ and $u^0\left(z',\omega,\beta_3^0\right)$ is determined by (42).

The minimum value of $\delta u(z,\omega)$ satisfies $\partial\delta u(z,\omega)/\partial\omega=0$, $R\left[\partial^2\delta u(z,\omega)/\partial\omega^2\right]>0$, so

$$\delta\beta_3=\exp\left[\int_{-\infty}^{+\infty}\left(-\frac{1}{G}\frac{\partial G}{\partial\omega}-\frac{3}{\omega}-\frac{1}{u^0}\frac{\partial u^0}{\partial\omega}\right)d\omega\right] \tag{45}$$

Next, we take the higher-order nonlinear effect into account. Constructing another iteration related to $\delta\gamma$: $\gamma = \gamma^0 + \delta\gamma$, $u(z,\omega) = u^0(z,\omega) + \delta u(z,\omega)$ and repeating the above process, we get

$$\delta\gamma \approx \exp\left[\int_{-\infty}^{+\infty}\left(-\frac{1}{G}\frac{\partial G}{\partial\omega} - \frac{3is}{1-3is\omega} - \frac{1}{u^0}\frac{\partial u^0}{\partial\omega}\right)d\omega\right] \tag{46}$$

Now, we can simulate the pulse shape affected by high-order dispersive and nonlinear effects. Assume $L_D = t_0^2/|\beta_2|$ and $u(0,t) = \int_{-\infty}^{+\infty} u(0,\omega)\exp(-i\omega t)d\omega = u_0\exp\left(-t^2/t_0^2/2\right)$.

Firstly, we see what will be induced by the above items $\delta\beta_3$ and $\delta\gamma$. To extrude their impact, we choose the other parameters to be small values in **Figures 4** and **5**. The deviation between the red and the black lines in **Figure 4(a)** indicates the impact of $\delta\beta_3$ and $\delta\gamma$; that is, they induce the pulse's symmetrical split. This split does not belong to the SPM-induced broadening oscillation spectral or β_3-induced oscillation in the tailing edge of the pulse, because here γ is very small and $\beta_3 = 0$ [3]. The self-steepening effect attributing to *is* $\partial\left(|u|^2u\right)/\partial t$ is also shown explicitly in the black line. When we reduce the *s* value to 0.0001 in (b), the split pulse's symmetry is improved.

Is the pulse split in **Figure 4(a)** caused by $\delta\beta_3$ or $\delta\gamma$? The red lines in **Figure 5** describe the evolution of pulse affected by the very small second-order dispersion and nonlinear (including self-steepening) coefficients. Here, $\delta\beta_3$ induces the pulse's symmetrical split, and the maximum peaks of split pulse alter and vary from the spectral central to the edge and to the central again. Therefore, its effect is equal to that of the fourth-order dispersion β_4 [33, 34, 3].

From the deviation between the red and black lines in **Figure 5**, we can also detect the impact of $\delta\gamma$. It only accelerates the pulse's split when the self-steepening effect is ignored (s = 0 in **Figure 5(a)**). This is similar to the self-phase modulation-broadening spectral and oscillation. The high nonlinear γ accelerating pulse's split is validated in [35, 36]. If $s \neq 0$ (**Figure 5(b)**), $\delta\gamma$ simultaneously leads to the split pulse's redshift.

Generally, we do not take $\delta\gamma$ into account, so we should clarify in which case it creates impact. Compared (c) with (b) in **Figure 5**, the red lines change little means that $\delta\beta_3$ has a tiny relationship with γ. But with the increase of γ (**Figure 5(c)**), the

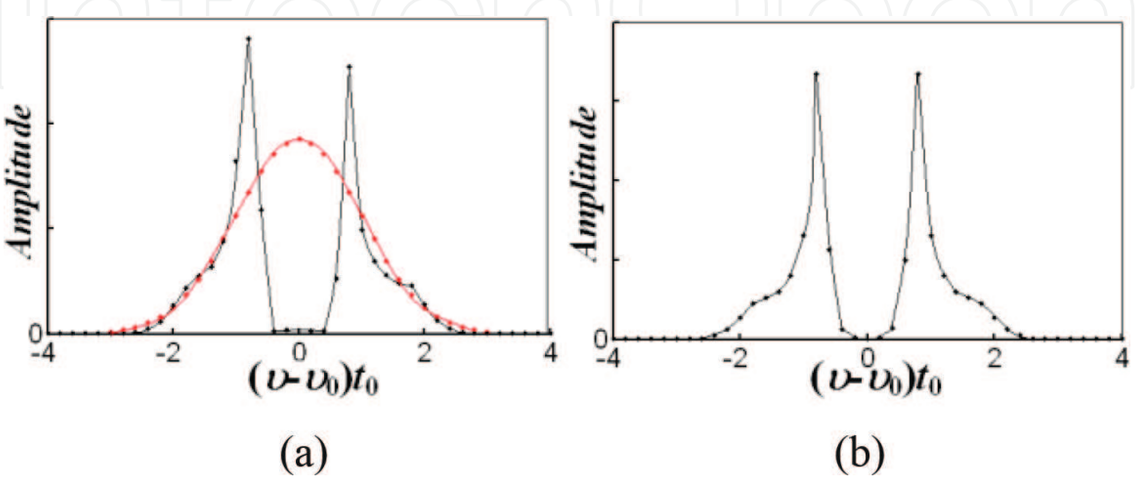

Figure 4.
The pulse shapes with and without $\delta\beta_3$ and $\delta\gamma$. The red line: without $\delta\beta_3$ and $\delta\gamma$; the black line: with $\delta\beta_3$ and $\delta\gamma$. $\nu = \omega/2/\pi$, $\beta_3^0 = 0$ $(\mathrm{ps}^3/\mathrm{km})$, $\gamma = 1.3\times10^{-2}(/\mathrm{km/W})$, $t_0 = 80(\mathrm{fs})$, $z = 3.7\times t_0^2/|\beta_2|$, $\beta_2 = -21.7/150(\mathrm{ps}^2/\mathrm{km})$, $u_0 = |\beta_2|/\gamma/t_0^2$. (a) s = *0.01 and (b)* s = *0.0001.*

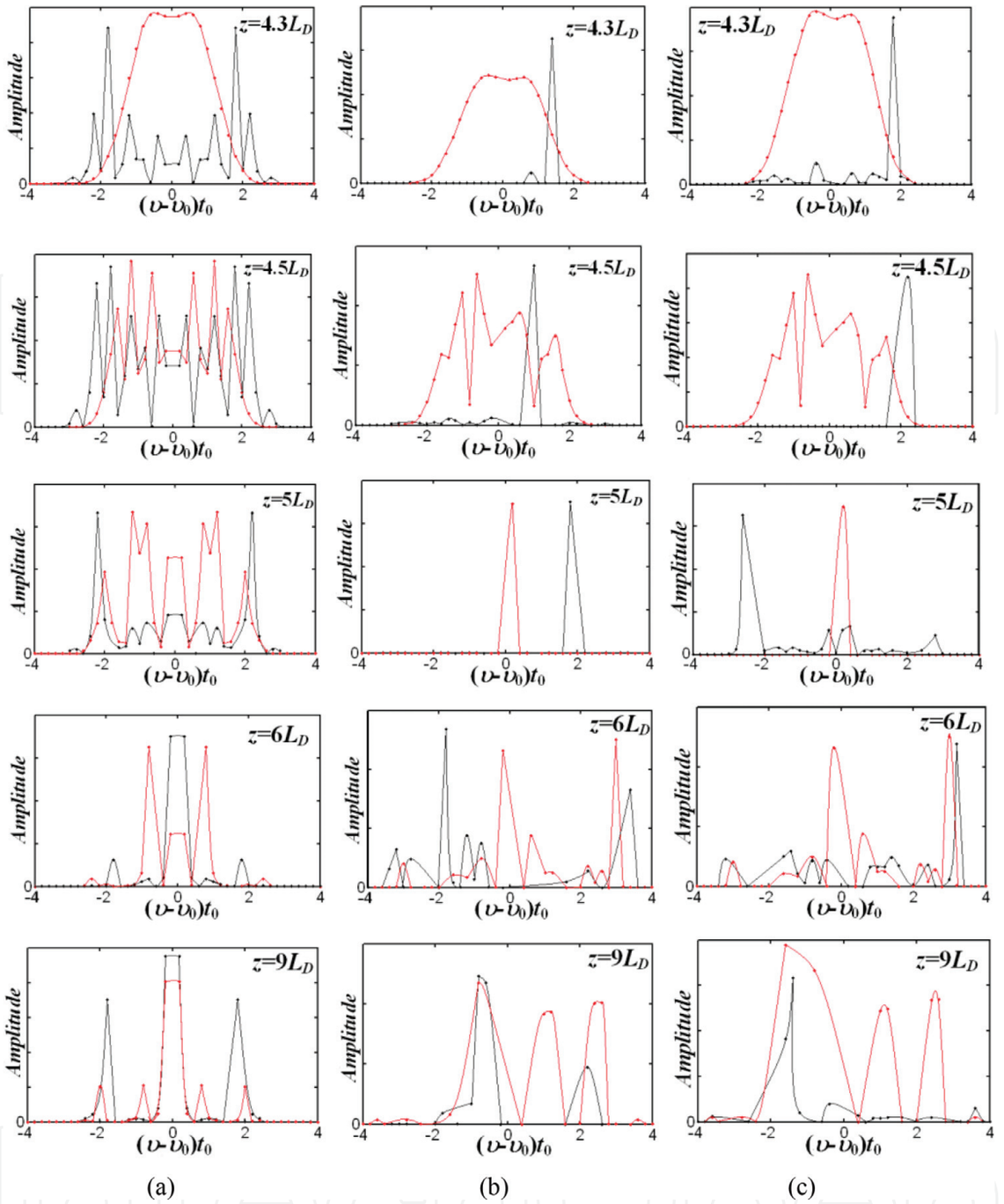

Figure 5.
The evolutions of pulse. The red line: without $\delta\gamma$; the black line: with $\delta\beta_3$ and $\delta\gamma$. (a) $s = 0$, $\gamma = 1.3 \times 10^{-4}$(/km/W); (b) $s = 0.01$, $\gamma = 1.3 \times 10^{-4}$(/km/W); (c) $s = 0.01$, $\gamma = 1.3$(/km/W). Other parameters are the same as ***Figure 4****.*

split pulse's redshift is strengthened, so $\delta\gamma$ has a relationship with γ. In **Figure 6**, the pulse is not split until $z = 9\ L_D$, and the black line with $\delta\gamma$ is completely overlapped by the red line without $\delta\gamma$, so the high second-order dispersion β_2 results in the impact of $\delta\gamma$ covered and the impact of $\delta\beta_3$ weakened. Therefore, only in the zero-dispersion regime, $\delta\gamma$ should be taken into account in the simulation of pulse shape.

So, we can utilize $\delta\beta_3$ to determine the fourth-order dispersion coefficient β_4. Fiber parameters are listed in **Table 1**. The process is shown in **Figure 7**, and the dispersion operator including β_4 is $\hat{D} = \frac{i}{2}\omega^2\beta_2 - \frac{i}{6}\omega^3\beta_3 + \frac{i}{24}\omega^4\beta_4$.

Table 2 is the average of β_4. They are different from those determined by FWM or MI where β_4 is related to power and broadening frequency [35, 36]. By our method, the fourth-order dispersion is also a function of distance, and every type of

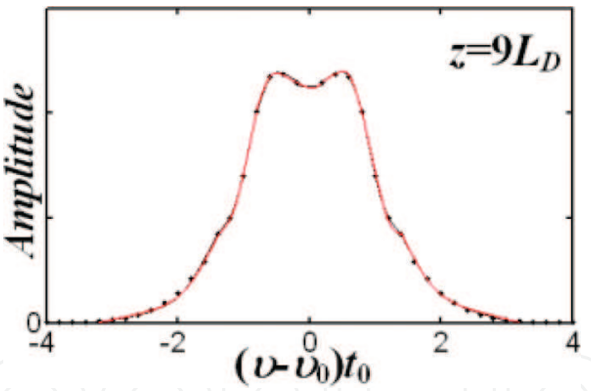

Figure 6.
The pulse shapes with and without $\delta\gamma$. $\beta_2 = -21.7(\mathrm{ps}^2/\mathrm{km})$, $s = 0.01$, $\gamma = 1.3$ $(/\mathrm{km/W})$. Other parameters are the same as ***Figure 5****.*

	a (dB/km)	γ (/km/W)	s	β_2 (ps^2/km)	β_3 (ps^3/km)
DCF	0.59	5.5	0.01	110	0.1381
NZDSF	0.21	2.2	0.01	−5.6	0.115
SMF	0.21	1.3	0.01	−21.7	−0.5

Table 1.
Fiber parameters.

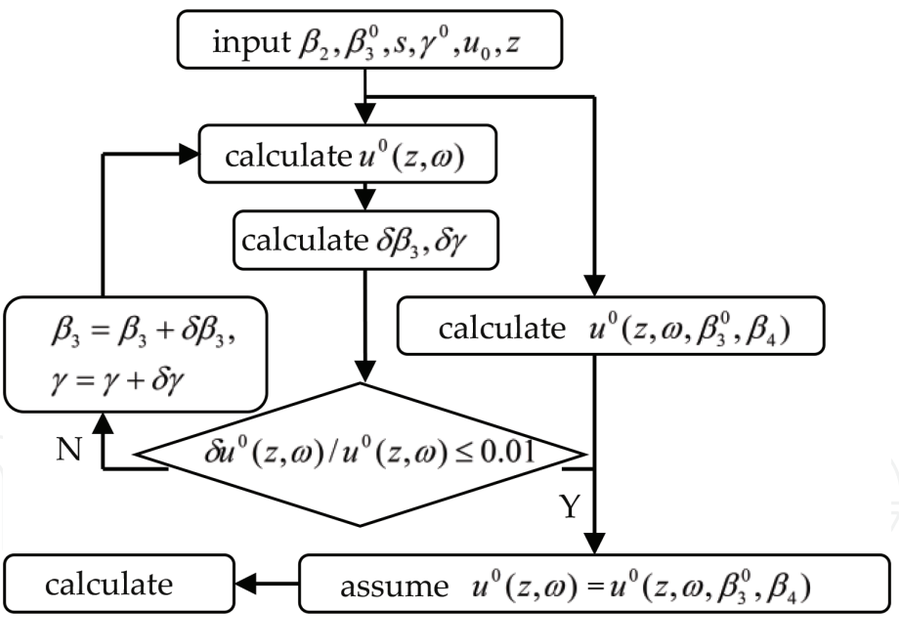

Figure 7.
The process of calculating β_4.

	$Z = 1.5L_D$	$Z = 5L_D$	$Z = 50L_D$
DCF	0.0003	0.00035	0.00032
NZDSF	0.0022	0.003	0.0032
SMF	0.0012	0.002	0.0025

Units (ps^4/km).

Table 2.
The average.

fibers has its special average β_4 which reveals the characteristic of fibers. These values are similar to those experiment results in highly nonlinear fibers [35, 36]. Although we take the higher-order nonlinear effect $\delta\gamma$ into account which upgrades the pulse's symmetrical split and redshift, the items *is* $\partial\left(|u|^2u\right)/\partial t$ and $i\delta\gamma \exp(-2\alpha z)|u|^2u$ have a very tiny contribution to β_4, only 10^{-26} ps^4/km quantity order for the typical SMF. Here, the impact of $\delta\gamma$ is hidden by the relative strong β_2.

4. Traveling wave solution of NLSE for ASE noise

4.1 The in-phase and quadrature components of ASE noise

The field including the complex envelopes of signal and ASE noise is:

$$U(z,t) = \sum_{l=1}^{N} [u_l(z,t) + A_l(z,t)] \exp(-i\omega_l t) \tag{47}$$

where $u_l(z,t)$ and $A_l(z,t)$ are the complex envelopes of signal and ASE noise, respectively [37, 38]. N is the channel number. ASE noise generated in erbium-doped fiber amplifiers (EDFAs) is $A_l(0,t) = A_{lR}(0,t) + iA_{lI}(0,t)$, $A_{lR}(0,t)$ and $A_{lI}(0,t)$ are statistically real independent stationary white Gaussian processes, and $\langle A_{lR}(0,t+\tau)A_{lR}^*(0,t)\rangle = \langle A_{lI}(0,t+\tau)A_{lI}^*(0,t)\rangle = n_{sp}hv_l(G_l-1)\Delta v_l\delta(\tau)$. In the complete inversion case, $n_{sp} = 1$. h is the Planck constant. G_l is the gain for channel l.

Substituting Eq. (47) into (1), we can get the equation that $A_l(z,t)$ satisfies:

$$\begin{aligned} i\frac{\partial A_l(z,t)}{\partial z} = \frac{\beta_2}{2}\left(-\omega_l^2 + \frac{\partial^2}{\partial t^2} - i2\omega_l\frac{\partial}{\partial t}\right)A_l(z,t) - \\ \gamma(z)\exp(-2\alpha z)\left|\sum_{j=1}^{N}u_j(z,t) + A_j(z,t)\right|^2 A_l(z,t) \end{aligned} \tag{48}$$

So, the in-phase and quadrature components of ASE noise obey:

$$\begin{aligned} \frac{\partial A_{lR}(z,t)}{\partial z} = -\beta_2\omega_l\frac{\partial A_{lR}(z,t)}{\partial t} + \frac{1}{2}\beta_2\frac{\partial^2 A_{lI}(z,t)}{\partial t^2} - \\ \frac{1}{2}\beta_2\omega_l^2 A_{lI} - \gamma\exp(-2\alpha z)\left|\sum_{j=1}^{N}u_j(z,t) + A_j(z,t)\right|^2 A_{lI} \end{aligned} \tag{49}$$

$$\begin{aligned} \frac{\partial A_{lI}(z,t)}{\partial z} = -\beta_2\omega_l\frac{\partial A_{lI}(z,t)}{\partial t} - \frac{1}{2}\beta_2\frac{\partial^2 A_{lR}(z,t)}{\partial t^2} + \frac{1}{2}\beta_2\omega_l^2 A_{lR}(z,t) + \\ \gamma\exp(-2\alpha z)\left|\sum_{j=1}^{N}u_j(z,t) + A_j(z,t)\right|^2 A_{lR} \end{aligned} \tag{50}$$

We now seek their traveling wave solution by taking [37] $A_{lR} = \phi(\xi)$, $A_{lI} = \varphi(\xi)$, and $\xi = t - cz$.

Then, (49) and (50) are converted into

$$\phi'(\beta_2\omega_l - c) = -\left[\frac{1}{2}\beta_2\omega_l^2 + \gamma\exp(-2\alpha z)\left|\sum_{j=1}^{N}u_j(z,t) + A_j(z,t)\right|^2\right]\varphi + \frac{1}{2}\beta_2\varphi'' \tag{51}$$

$$\varphi'(\beta_2\omega_l - c) = \left[\frac{1}{2}\beta_2\omega_l^2 + \gamma\exp(-2\alpha z)\left|\sum_{j=1}^{N} u_j(z,t) + A_j(z,t)\right|^2\right]\phi - \frac{1}{2}\beta_2\phi'' \quad (52)$$

(52) is differentiated to ξ

$$\varphi''(\beta_2\omega_l - c) = \left[\frac{1}{2}\beta_2\omega_l^2 + \gamma\exp(-2\alpha z)\left|\sum_{j=1}^{N} u_j(z,t) + A_j(z,t)\right|^2\right]\phi' - \frac{1}{2}\beta_2\phi''' \quad (53)$$

Replacing ϕ' and ϕ''' in (53) with (51) and the differential of (51), there are

$$\phi''(\beta_2\omega_l - c)^2 = -\left[\tfrac{1}{2}\beta_2\omega_l^2 + \gamma\exp(-2\alpha z)\left|\sum_{j=1}^{N} u_j(z,t) + A_j(z,t)\right|^2\right]^2\phi + \beta_2\left[\frac{1}{2}\beta_2\omega_l^2 + \gamma\exp(-2\alpha z)\left|\sum_{j=1}^{N} u_j(z,t) + A_j(z,t)\right|^2\right]\phi'' + \frac{1}{4}\beta_2^2\phi^{(4)} \quad (54)$$

From (51) and (54), we can easily obtain

$$\varphi = B\left\{\left[\beta_2\omega_l^2/2 + \gamma\exp(-2\alpha z)\left|\sum_{j=1}^{N} u_j(z,t) + A_j(z,t)\right|^2\right]\cos k\xi + \beta_2 k^2/2\cdot\cos k\xi\right\}/(\beta_2\omega_l - c)/k \quad (55)$$

$$\varphi = B\sin k\xi \quad (56)$$

and

$$B = A_{lR}(0,t)(\beta_2\omega_l - c)k/\left\{\left[\beta_2\omega_l^2/2 + \gamma\exp(-2\alpha z)\left|\sum_{j=1}^{N} u_j(z,t) + A_j(z,t)\right|^2\right]\cos kt + \beta_2 k^2/2\cdot\cos kt\right\} \quad (57)$$

$$c = \pm\left\{\beta_2^2k^2/4 + \left[\beta_2\omega_l^2/2 + \gamma\exp(-2\alpha z)^2\left|\sum_{j=1}^{N} u_j(z,t) + A_j(z,t)\right|^2\right]/k^2 + \beta_2^2\omega_l^2/2 + \gamma\beta_2\exp(-2\alpha z)\left|\sum_{j=1}^{N} u_j(z,t) + A_j(z,t)\right|^2\right\}^{1/2} + \beta_2\omega_l \quad (58)$$

$$k = \arcsin(A_{lI}(0,t)/B)/t \quad (59)$$

In the above calculation process, B, c, and k should be regarded as constants, and A_{lR}, A_{lI} are the functions of the solo variable ξ, respectively.

4.2 Probability density function of ASE noise

Because A_{lR} and A_{lI} have been solved, the time differentials of (49) and (50) can be calculated. Thus, the stochastic differential equations (ITO forms) around A_{lR} and A_{lI} are

$$\frac{\partial A_{lR}(z,t)}{\partial z} = f(A_{lR}(z,t)) + g(A_{lR}(z,t))A_{lR,z=0} \tag{60}$$

$$\frac{\partial A_{lI}(z,t)}{\partial z} = f^{'}(A_{lI}(z,t)) + g^{'}(A_{lI}(z,t))A_{lI,z=0} \tag{61}$$

Here,

$$f(A_{lR}(z,t)) = \beta_2 k\omega_l \sqrt{\left[B\frac{\beta_2\omega_l^2/2+\gamma\exp(-2\alpha z)\left|\sum_{j=1}^{N}u_j(z,t)+A_j(z,t)\right|^2+\beta_2k^2/2}{(\beta_2\omega_l-c)k}\right]^2 - A_{lR}^2(z,t)} \tag{62}$$

$$g(A_{lR}(z,t)) = -\frac{(\beta_2\omega_l - c)k}{A_{lR,z=0}} \sqrt{\left[B\frac{\beta_2\omega_l^2/2+\gamma\exp(-2\alpha z)\left|\sum_{j=1}^{N}u_j(z,t)+A_j(z,t)\right|^2+\beta_2k^2/2}{(\beta_2\omega_l-c)k}\right]^2 - A_{lR}^2(z,t)} \tag{63}$$

$$f^{'}(A_{lI}(z,t)) = -\beta_2 k\omega_l\sqrt{B^2 - A_{lI}^2(z,t)} \tag{64}$$

$$g'(A_{lI}(z,t)) = \left[B\frac{\beta_2\omega_l^2/2+\gamma\exp(-2\alpha z)\left|\sum_{j=1}^{N}u_j(z,t)+A_j(z,t)\right|^2+\beta_2k^2/2}{(\beta_2\omega_l-c)k}\right]^2 \frac{(\beta_2\omega_l - c)k}{BA_{lI,z=0}}\sqrt{B^2 - A_{lI}^2(z,t)} \tag{65}$$

Now, they can be regarded as the stationary equations, and we can gain their probabilities according to Sections (7.3) and (7.4) in [39]. By solving the corresponding Fokker-Planck equations of (60) and (61), the probabilities of ASE noise are

$$p_{lR} = \frac{C}{[g(A_{lR})]^2}\exp\left[2\int_{-\infty}^{A_{lR}}\frac{f(s)}{[g(s)]^2}ds\right] \tag{66}$$

$$p_{lI} = \frac{C'}{[g'(A_{lI})]^2}\exp\left[2\int_{-\infty}^{A_{lI}}\frac{f'(s)}{[g'(s)]^2}ds\right] \tag{67}$$

C, C' are determined by $\int_{-\infty}^{+\infty} pdp = 1$. Compared with [40], these probabilities of ASE noise take dispersion effect into account. This is the first time that the p.d.f. of ASE noise simultaneously including dispersion and nonlinear effects is presented.

(66) and (67) are efficient in the models of Gaussian and correlated non-Gaussian processes as our (49) and (50). Obviously, the Gaussian distribution has been distorted. They are no longer symmetrical distributions, and both have phase shifts consistent with [40], and as its authors have expected that "if the dispersion

effect was taken into account, the asymmetric modulation side bands occur." The reasons are that item $-i\beta_2\omega_l \frac{\partial}{\partial t} A_l(z,t)$ in (48) brings the phase shift and item $\frac{\beta_2}{2}\frac{\partial^2}{\partial t^2} A_l(z,t)$ brings the expansion and induces the side bands, the self-phase modulation effects, and the cross-phase modulation effects. Their synthesis impact is amplified by (66) and (67) and results in the complete non-Gaussian distributions.

5. Conclusion

NLSE is solved with small-signal analyses for the analyses of MI, and it can be broadened to all signal formats. The equation can be solved by introducing the Green function in the time domain, and it is used as the tool for the estimations of high-order dispersion and nonlinear coefficients. For the conventional fibers, SMF, NZDSF, and DCF, the higher-order nonlinear effect contribution to β_4 can be neglected. This can be deduced that each effect has less impact for another coefficient's estimation. The Green function can also be used for the solving of 3 + 1 dimension NLSE.

By the traveling wave methods, the p.d.f. of ASE noise can be obtained, and it provides a method for the calculation of ASE noise in WDM systems. So, the properties of MI, pulse fission, coefficient value, and ASE noise's probability density function are also discussed for demonstrations of the theories.

Author details

Jing Huang
Physics Department, South China University of Technology, Guangzhou, China

*Address all correspondence to: jhuang@scut.edu.cn

References

[1] Hasegawa A, Matsumoto M, Kattan PI. Optical Solitons in Fibers. 3rd ed. New York: Springer-Verlag; 2000

[2] Brandt-Pearce M, Jacobs I, Shaw JK. Optimal input Gaussian pulse width for transmission in dispersive nonlinear fiber. Journal of the Optical Society of America B. 1999;**16**:1189-1196. DOI: 10.1364/JOSAB.16.001189

[3] Agrawal GP. Nonlinear Fiber Optics. 4th ed. San Diego, CA: Academic; 2007

[4] Kodama Y, Wabnitz S. Analytical theory of guiding center nonreturn to zero and return to zero signal transmission in normally dispersive nonlinear optical fibers. Optics Letters. 1995;**20**:2291-2293. DOI: 10.1364/OL.20.002291

[5] Surján PR, Ángyán J. Perturbation theory for nonlinear time-independent Schrödinger equations. Physical Review A–Physical Review Journals. 1983;**28**: 45-48. DOI: 10.1103/PhysRevA.28.45

[6] Peddanarappagari KV, Brandt-Pearce M. Volterra series transfer function of single-mode fibers. Journal of Lightwave Technology. 1997;**15**: 2232-2241. DOI: 10.1109/50.643545

[7] Serkin VN, Hasegawa A. Novel soliton solutions of the nonlinear Schrödinger equation model. Physical Review Letters. 2000;**85**:4502-4505. DOI: 10.1103/PhysRevLett.85.4502

[8] Cerda SC, Cavalcanti SB, Hickmann JM. A variational approach of nonlinear dissipative pulse propagation. European Physical Journal D. 1998;**1**:313-316. DOI: 10.1007/s100530050

[9] Roy S, Bhadra SK. Solving soliton perturbation problems by introducing Rayleigh's dissipation function. Journal of Lightwave Technology. 2008;**26**: 2301-2322. DOI: 10.1109/JLT.2008.922305

[10] Chang Q, Jia E, Suny W. Difference schemes for solving the generalized nonlinear Schrodinger equation. Journal of Computational Physics. 1999;**148**: 397-415. DOI: 10.1006/jcph.1998.6120

[11] Bosco G, Carena A, Curri V, Gaudino R, Poggiolini P, Bendedetto S. Suppression of spurious tones induced by the split-step method in fiber systems simulation. IEEE Photonics Technology Letters. 2000;**12**:489-491. DOI: 10.1109/68.841262

[12] Sinkin V, Holzlohner R, Zweck J, Menyuk CR. Optimization of the split-step Fourier method in modeling optical-fiber communication systems. Journal of Lightwave Technology. 2003; **21**:61-68. DOI: 10.1109/JLT.2003.808628

[13] Liu X, Lee B. A fast method for nonlinear Schrodinger equation. IEEE Photonics Technology Letters. 2003;**15**: 1549-1551. DOI: 10.1109/LPT.2003.818679

[14] Premaratne M. Numerical simulation of nonuniformly time-sampled pulse propagation in nonlinear fiber. Journal of Lightwave Technology. 2005;**23**:2434-2442. DOI: 10.1109/JLT.2005.850770

[15] Dabas B, Kaushal J, Rajput M, Sinha RK. Nonlinear pulse propagation in chalcogenide As2Se3 glass photonic crystal fiber using RK4IP method. Applied Optics. 2011;**50**:5803-5811. DOI: 10.1364/AO.50.005803

[16] Pedersen MEV, Ji C, Chris X, Rottwitt K. Transverse field dispersion in the generalized nonlinear Schrodinger equation: Four wave mixing in a higher order mode fiber.

Journal of Lightwave Technology. 2013; **31**:3425-3431. DOI: 10.1109/ JLT.2013.2283423

[17] Deiterding R, Glowinski R, Oliver H, Poole S. A reliable split-step Fourier method for the propagation equation of ultra-fast pulses in single-mode optical fibers. Journal of Lightwave Technology. 2013;**31**:2008-2017. DOI: 10.1109/JLT.2013.2262654

[18] Choudhuri A, Porsezian K. Impact of dispersion and non-Kerr nonlinearity on the modulational instability of the higher-order nonlinear Schrodinger equation. Physical Review A. 2012;**85**: 033820. DOI: 10.1103/ PhysRevA.85.033820

[19] Huang J, Yao J. Small-signal analysis of cross-phase modulation instability in lossy fibres. Journal of Modern Optics. 2005;**52**:1947-1955. DOI: 10.1080/ 09500340500106717

[20] Wang J, Petermann K. Small signal analysis for dispersive optical fiber communication systems. Journal of Lightwave Technology. 1992;**10**:96. DOI: 10.1109/50.108743

[21] Huang W, Hong J. A coupled-mode analysis of modulation instability in optical fibers. Journal of Lightwave Technology. 1992;**10**:156-162. DOI: 10.1109/50.120570

[22] Meslener GJ. Chromatic dispersion induced distortion of modulated monochromatic light employing direct detection. IEEE Journal of Quantum Electronics. 1984. DOI: QE-20: 1208-1216. DOI:10.1109/ JQE.1984.1072286

[23] Koyama F, Suematsu Y. Analysis of dynamic spectral width of dynamic-single-mode (DSM) lasers and related transmission bandwidth of single-mode fibers. IEEE Journal of Quantum Electronics. 1985. DOI: QE-21:292-297. DOI:10.1109/JQE.1985.1072653

[24] Rchraplyvy A, Tkach RW, Buhl LL, Alferness RC. Phase modulation to amplitude modulation conversion of CW laser light in optical fibres. Electronics Letters. 1988;**22**:409-412. DOI: 10.1049/el:19860279

[25] Grudihin AB, Dianov EM, Korobkin DV, Prokhorov AM, Serkin VN. Decay of femtosecond pulses in single-mode fiber-optic waveguides. JETP Letters. 1987;**46**:221-225

[26] Agrawal GP, Baldeck PL, Alfano RR. Modulation instability induced by cross-phase modulation in optical fibers. Physical Review A. 1989;**39**:3406-3413. DOI: 10.1103/PhysRevA.39.3406

[27] Ciaramella E, Tamburrini M. Modulation instability in long amplified links with strong dispersion compensation. IEEE Photonics Technology Letters. 1999;**11**:1608-1610. DOI: 10.1109/ 68.806862

[28] Huang J, Yao J. Analysis of cross-phase modulation in WDM systems. Journal of Modern Optics. 2005;**52**: 1819-1825. DOI: 10.1080/ 09500340500092016

[29] Cartaxo AVT. Impact of modulation frequency on crossphase modulation effect in intensity modulation-direct detection WDM systems. IEEE Photonics Technology Letters. 1998;**10**: 1268-1270. DOI: 10.1109/68.705612

[30] Huang J, Yao J, Degang X. Green function method for the time domain simulation of pulse propagation. Applied Optics. 2014;**53**(16):-20

[31] Shen YR. The Principles of Nonlinear Optics. Hoboken, NJ: John Wiley & Sons, Inc; 1984

[32] Huang J, Yao J. Estimation of the fourth-order dispersion coefficient β_4. Chinese Optics Letters. 2012;**10**: 101903-101903. DOI: 10.3788/ COL201210.101903

[33] Capmany J, Pastor D, Sales S, Ortega B. Effects of fourth-order dispersion in very high-speed optical time-division multiplexed transmission. Optics Letters. 2002;**27**:960-962. DOI: 10.1364/OL.27.000960

[34] Igarashi K, Saito S, Kishi M, Tsuchiya M. Broad-band and extremely flat super-continuum generation via optical parametric gain extended spectrally by fourth-order dispersion in anomalous-dispersion-flattened fibers. IEEE Journal of Selected Topics in Quantum Electronics. 2002;**8**:521-526. DOI: 10.1109/JSTQE.2002.1016355

[35] Gholami F, Chavez Boggio JM, Moro S, Alic N, Radic S. Measurement of ultra-low fourth order dispersion coefficient of nonlinear fiber by distant low-power FWM. IEEE Photonics Society Summer Topical Meeting Series. 2010;**2010**:162-163. DOI: 10.1109/PHOSST.2010.5553630

[36] Marhic ME, Wong KK-Y, Kazovsky LG. Wide-band tuning of the gain spectra of one-pump fiber optical parametric amplifiers. IEEE Journal of Selected Topics in Quantum Electronics. 2004;**10**:1133-1141. DOI: 10.1109/JSTQE.2004.835298

[37] Gui M, Jing H. Statistical analyses of ASE noise. Optics and Photonics Journal. 2017;**7**:160-169. DOI: 10.4236/opj.2017.710016

[38] Nichel J, Schurmann HW, Serov VS. Some elliptic travelling wave solution to the Nonikov-Vesela equation. In: Proceedings of the International Conference on Days on Diffraction, DD2005; 2005, 28–01; 2005. pp. 177-186

[39] Primak S, Kontorovich V, Lyandres V. Stochastic Method and Their Applications to Communications. Chichester, UK: John Wiley & Sons; 2004. Chap. 7. DOI:10.1002/0470021187

[40] Dlubek MP, Phillips AJ, Larkins EC. Nonlinear evolution of Gaussian ASE noise in ZMNL fiber. Journal of Lightwave Technology. 2008;**26**: 891-898. DOI: 10.1109/JLT.2008.917373